THE JOURNAL OF BIOLOGICAL CHEMISTRY VOL. 283, NO. 27, pp. 18665–18677, July 4, 2008

Molecular Determinants of Sphingomyelin Specificity of a Eukaryotic Pore-forming Toxin*[S]

Received for publication, October 23, 2007, and in revised form, April 24, 2008 Published, JBC Papers in Press, April 28, 2008, DOI 10.1074/jbc.M708747200

Biserka Bakrač[‡1], Ion Gutiérrez-Aguirre[‡1,2], Zdravko Podlesek[‡], Andreas F.-P. Sonnen[§3], Robert J. C. Gilbert[§4], Peter Maček[‡], Jeremy H. Lakey[¶5,6], and Gregor Anderluh[‡5,7]

From the [‡]Department of Biology, Biotechnical Faculty, University of Ljubljana, Večna pot 111, 1000 Ljubljana, Slovenia, [§]Division of Structural Biology, Wellcome Trust Centre for Human Genetics, University of Oxford, Roosevelt Drive, Oxford OX3 7BN, United Kingdom, and [¶]Institute of Cell and Molecular Biosciences, University of Newcastle upon Tyne, Framlington Place, NE2 4HH Newcastle upon Tyne, United Kingdom

Sphingomyelin (SM) is abundant in the outer leaflet of the cell plasma membrane, with the ability to concentrate in so-called lipid rafts. These specialized cholesterol-rich microdomains not only are associated with many physiological processes but also are exploited as cell entry points by pathogens and protein toxins. SM binding is thus a widespread and important biochemical function, and here we reveal the molecular basis of SM recognition by the membrane-binding eukaryotic cytolysin equinatoxin II (EqtII). The presence of SM in membranes drastically improves the binding and permeabilizing activity of EqtII. Direct binding assays showed that EqtII specifically binds SM, but not other lipids and, curiously, not even phosphatidylcholine, which presents the same phosphorylcholine headgroup. Analysis of the EqtII interfacial binding site predicts that electrostatic interactions do not play an important role in the membrane interaction and that the two most important residues for sphingomyelin recognition are Trp^{112} and Tyr^{113} exposed on a large loop. Experiments using site-directed mutagenesis, surface plasmon resonance, lipid monolayer, and liposome permeabilization assays clearly showed that the discrimination between sphingomyelin and phosphatidylcholine occurs in the region directly below the phosphorylcholine headgroup. Because the characteristic features of SM chemistry lie in this subinterfacial region, the recognition mechanism may be generic for all SM-specific proteins.

Sphingomyelin (SM)[8] is an important eukaryotic membrane lipid, located for the most part in the outer leaflet of the plasma membrane in the form of specialized cholesterol-rich microdomains, so-called lipid rafts (1, 2). Many pathogens and toxic proteins employ lipid rafts to invade cells (3, 4), but currently little is known about the molecular details of the recognition mechanism of the lipid components present in the rafts. In the particular case of SM, the specific recognition occurs even though SM exposes the same phosphorylcholine headgroup as the other abundant lipid, phosphatidylcholine. SM-binding proteins are currently exploited as specific markers for cellular SM (5) and are used to identify other proteins involved in sphingolipid metabolism (6).

Actinoporins are extremely potent cytolysins produced exclusively by sea anemones (7, 8). They may be used to capture prey, in intraspecific aggression, or in preventing adhesion of other organisms (7, 9). The two most studied representatives are EqtII, isolated from the sea anemone *Actinia equina*, and sticholysin II (StII) from *Stichodactyla helianthus*. Actinoporins constitute a family of conserved proteins that cause hemolysis of red blood cells by colloid-osmotic lysis and exhibit cytolytic activity against various cell lines (7, 10–12). Even the most distant members of the family share more than 60% sequence identity and the available three-dimensional structures of EqtII and StII are nearly superimposable (13–15). The structure is composed of a tightly folded β-sandwich flanked by two α-helices (13–15). The N-terminal helix is used for transmembrane pore formation (16, 17). Hence actinoporins belong to the class of α-helical pore-forming proteins and represent an important model for the study of protein-membrane interactions (18). The membrane-binding step is enabled by amino acid residues exposed on the loops located on one side of the β-sandwich (19–21). Interestingly, an equivalent site with similar amino acid residues is used by fungal fruit body lectins to selectively bind a Galβ1–3GalNAc disaccharide (Thomsen-Friedenreich antigen) present on glycoproteins of malignant cells (22, 23). Thus the archetypical actinoporin structural scaffold is widespread and is used for the specific binding to various molecules of the plasma membrane (24).

The membrane-lytic activity of actinoporins is highly SM-dependent (reviewed in Ref. 7), and it has been proposed that

* This work was supported in part by Grant P1-0207 from the Slovenian Research Agency. The costs of publication of this article were defrayed in part by the payment of page charges. This article must therefore be hereby marked "*advertisement*" in accordance with 18 U.S.C. Section 1734 solely to indicate this fact.

[S] The on-line version of this article (available at http://www.jbc.org) contains supplemental material and supplemental Table 1.

[1] These two authors contributed equally to this work.
[2] Recipient of a postdoctoral fellowship from the Basque government. Current address: Dept. of Plant Physiology and Biotechnology, National Inst. of Biology, Večna pot 111, 1000 Ljubljana, Slovenia.
[3] Recipient of a Wellcome Trust Structural Biology Studentship.
[4] A Royal Society University Research Fellow.
[5] Joint recipients of an International Research Development Award from the Wellcome Trust.
[6] Recipient of Wellcome Trust Equipment Grants 56232, 40422, and 55979.
[7] To whom correspondence should be addressed. Tel.: 386-1-423-33-88; Fax: 386-1-257-33-90; E-mail: gregor.anderluh@bf.uni-lj.si.

[8] The abbreviations used are: SM, sphingomyelin; Ac-SM, *N*-acetyl-D-*erythro*-sphingosylphosphorylcholine; BSA, bovine serum albumin; EqtII, equinatoxin II; IBS, interfacial binding site; LUV, large unilamellar vesicles; NBD, *N*-((2-(iodoacetoxy)ethyl)-*N*-methyl)amino-7-nitrobenz-2-oxa-1,3-diazole; DOPC, 1,2-dioleoyl-*sn*-glycero-3-phosphocholine; DPPC, 1,2-dipalmitoyl-*sn*-glycero-3-phosphocholine; PC, phosphatidylcholine; POC, phosphorylcholine; RU, response units; POPG, 1-palmitoyl-2-oleoyl-phosphatidylglycerol; StII, sticholysin II; mN, millinewton; GM1, Galβ1, 3GalNAcβ1, 4(NeuAcα2,3)Galβ1, 4Glc-ceramide.

SM plays a major role in the binding of the toxin to the membrane (25). This was supported by the recent discovery of a phosphorylcholine (POC) binding site on the surface of StII (15). However, some published data indicate that the addition of cholesterol to phosphatidylcholine (PC) liposomes also increases actinoporin permeabilizing activity (26–28). It thus remains to be determined whether the SM effect originates from a general influence of the physico-chemical properties of the membrane or is a result of specific binding. Lipid specificity has been poorly addressed in the available structural studies of actinoporins (13–15, 29, 30). Recently, however, it was shown by introducing a ^{19}F label on EqtII tryptophans that Trp^{112} participates in SM recognition, as it exhibits specific NMR chemical shift changes upon the addition of SM to PC micelles (31).

In this work we have tested the hypothesis that EqtII can specifically bind sphingomyelin both in solution and in lipid membranes. We show that EqtII is able to specifically bind SM but neither cholesterol nor phosphatidylcholine. We additionally show that the membrane-binding step is driven mainly by hydrophobic rather than electrostatic interactions and that the residues Trp^{112} and Tyr^{113} enable SM dependence.

EXPERIMENTAL PROCEDURES

Materials—1,2-Dioleoyl-*sn*-glycero-3-phosphocholine (DOPC), 1,2-dipalmitoyl-*sn*-glycero-3-phosphocholine (DPPC), 1,2-dipropionoyl-*sn*-glycero-3-phosphocholine, porcine brain SM, *N*-acetyl-D-*erythro*-sphingosylphosphorylcholine (Ac-SM), chicken egg SM, porcine brain ceramide, D-glucosyl-β-1,1′-*N*-stearoyl-D-*erythro*-sphingosine, D-galactosyl-β-1–1′-*N*-nervonoyl-D-*erythro*-sphingosine, D-lactosyl-β-1,1′-*N*-palmitoyl-D-*erythro*-sphingosine, ovine brain ganglioside G_{M1}, and cholesterol were from Avanti Polar Lipids (Alabaster, AL); 1-lauroyl-2-hydroxy-*sn*-glycero-3-phosphocho-

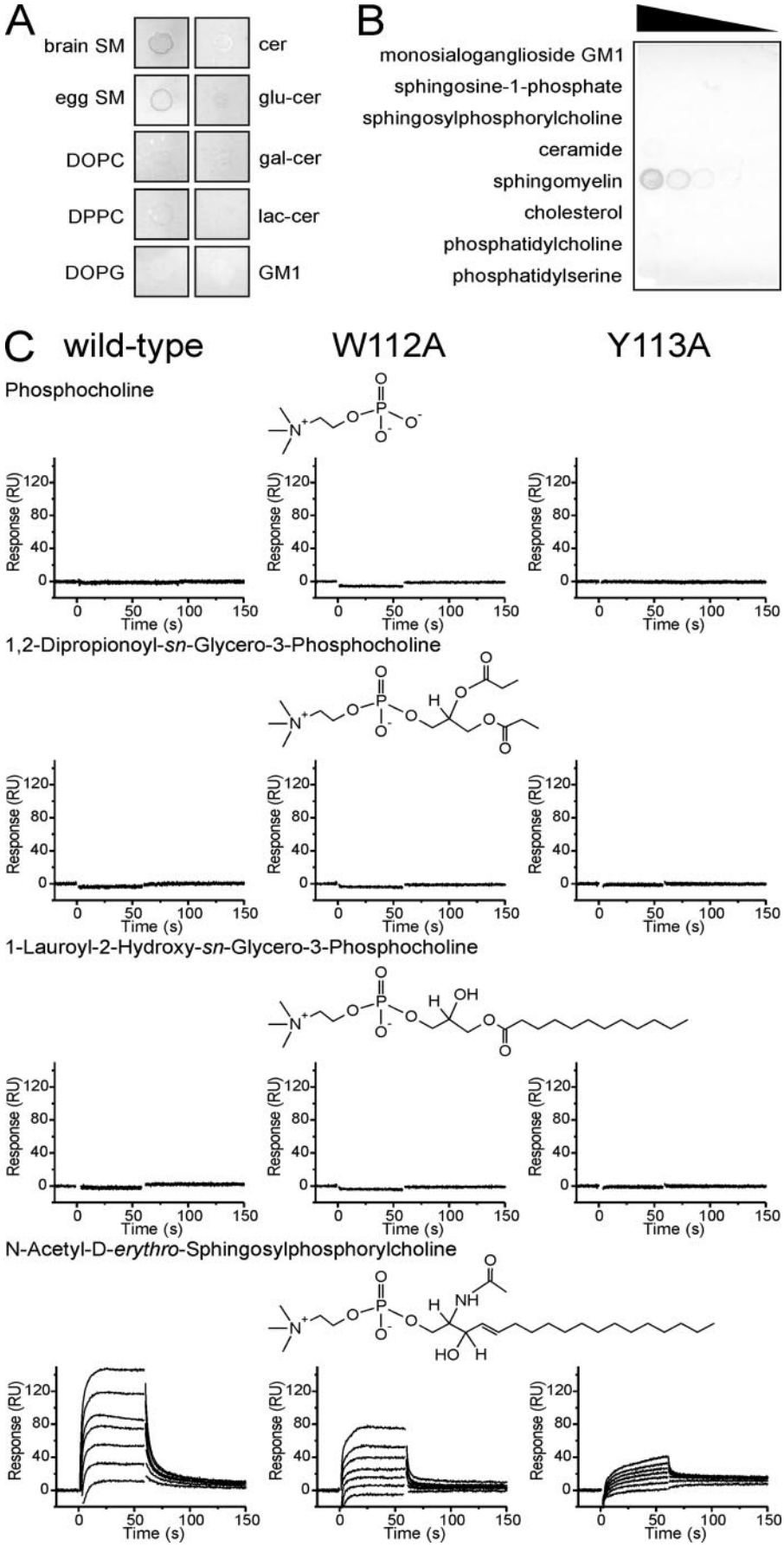

line was from Sigma. Bovine brain SM was used in all experiments unless stated otherwise. All other chemicals were from Sigma unless stated otherwise. Recombinant EqtII, mutants and histidine-tagged variants were prepared in *Escherichia coli* as described previously (19, 32). The tryptophan fluorescence and far UV circular dichroism spectra showed that mutations did not cause large structural changes.[9] EqtII G27C mutant was labeled with *N*-((2-(iodoacetoxy)ethyl)-*N*-methyl)amino-7-nitrobenz-2-oxa-1,3-diazole (NBD) as described (16). All reported lipid ratios are mol:mol ratios.

Liposome Preparations—Large unilamellar vesicles (LUV) of 100-nm diameter were prepared by extrusion of multilamellar vesicles as described previously (19). When using calcein, excess dye was removed by gel filtration through a small G-50 column. Permeabilization assays of calcein-loaded liposomes were conducted with a Jasco FP-750 spectrofluorometer in a 1.5-ml cuvette. Liposomes at 25 μM lipid concentration were stirred in 140 mM NaCl, 20 mM Tris-HCl, 1 mM EDTA, pH 8.5 (vesicle buffer), at 25 °C. The excitation wavelength was set to 485 nm, emission was followed at 520 nm, and both slits were set to 5 nm. Permeabilization was expressed as the percentage of maximal permeabilization obtained at the end of the assay by addition of detergent Triton X-100 to a final concentration of 2 mM.

Hemolysis and Preparation of Erythrocyte Ghosts—Hemolysis of human or bovine red blood cells was measured at room temperature by using a microplate reader (MRX, Dynex). Blood was washed several times with 130 mM NaCl, 20 mM Tris-HCl, pH 7.4 (erythrocyte buffer), and proteins were diluted 2-fold across the microtiter plate into a final volume of 100 μl of erythrocyte buffer. The same volume of erythrocyte suspension (A_{630} = 0.5) was added to each well, and hemolysis was monitored at 630 nm for 20 min at room temperature.

Erythrocyte ghosts were prepared from washed erythrocytes by lysing 50 μl of erythrocytes with 1400 μl of cold 5 mM Na_2HPO_4, pH 8.0, for 5 min on ice. Lysed erythrocytes were collected by centrifugation for 10 min at 14,000 × *g*. Ghosts were washed with the same buffer until all hemoglobin was removed, *i.e.* when a clear pellet was obtained that could subsequently be resuspended in a small volume of buffer.

Cholesterol was depleted from erythrocytes by incubation with 10 mM methyl-β-cyclodextrin for 30 min at 37 °C. SM was removed from erythrocytes by incubation with *Bacillus cereus* sphingomyelinase. 0.5 ml of washed erythrocytes was incubated with 2 units/ml *B. cereus* sphingomyelinase in the presence of 2 mM 1,10-phenanthroline in erythrocyte buffer for 60 min at 37 °C. Erythrocytes were washed extensively before use in hemolytic assay or ghost preparations. The removal of cholesterol and SM from erythrocyte membranes was confirmed by enzymatic tests for lipid concentration determination: phospholipids B (for choline-containing lipids) and free cholesterol C (for cholesterol) (both from Wako). Additionally, total lipid extracts were prepared from erythrocytes by the method of Bligh and Dyer (33) and analyzed by thin layer chromatography (TLC) to confirm both the removal of SM and cholesterol and that the amount of other lipids in the membrane was not altered. The TLC plates were stained with primulin and visualized under UV light.

Surface Plasmon Resonance Assay—Surface plasmon resonance (SPR) measurements were performed on a Biacore X (Biacore AB) at 25 °C. An L1 chip was equilibrated with vesicle buffer, and a liposome-coated chip surface was prepared as described previously (34). Proteins (0.5 μM) were injected over immobilized LUV for 2 min at 5 μl/min, and the dissociation was followed for 4 min. Erythrocyte ghosts were immobilized by using the same protocol to a final value of 1200 response units (RU). The concentration of EqtII was 50 nM for the binding assay employing erythrocyte ghosts. Blank injections were subtracted from sensorgrams to correct for the buffer contribution. The amount of stably inserted protein after 4 min of dissociation was determined from the sensorgrams and used to report in Figs. 3, *B* and *D*, and 4*D*.

Kinetic analysis of EqtII and mutant binding was performed as described above. Protein concentrations were adjusted so that the response did not exceed 300 RU. This enabled us to monitor only the initial binding to the liposomes and not the subsequent steps in the pore-forming mechanism (34). The data were globally fitted to a two-step binding model described in detail in Hong *et al.* (21). The first and last 10 s of the injection and the first 10 s of the dissociation were not included in the fit because of bulk refractive index changes and mixing effects (35).

Binding of lipid analogues to proteins was performed on a Biacore 2000 (Biacore AB). Wild-type EqtII or mutants were immobilized on the surface of a CM5 chip to ~4000 RU as recommended by the supplier (Biacore AB). The buffer used was 20 mM NaH_2PO_4, 140 mM NaCl, pH 7.0 (SPR buffer), and the flow rate was set to 40 μl/min. Association was followed for 1 min and dissociation for 3 min. Lipid analogues were dissolved as 50 mM stock solutions in SPR buffer. We could only perform a qualitative analysis for the Ac-SM, because it forms micelles at a concentration of 31 μM,[10] and hence we could not determine whether it bound as a monomer.

Lipid Monolayer Assay—The increase in the surface pressure of lipid monolayers of different compositions was measured with a MicroTrough-S system from Kibron (Helsinki, Finland) at room temperature. The aqueous subphase consisted of 500 μl of 10 mM Hepes, 200 mM NaCl, pH 7.5. Appropriate lipid mixtures, dissolved in chloroform:methanol (2:1, v/v), were gently spread over the subphase to create a monolayer with the

[9] G. Anderluh, unpublished data.

[10] I. Gutiérrez-Aguirre and G. Anderluh, unpublished data.

FIGURE 1. **Direct binding to SM.** *A* and *B*, dot-blot binding assay using some of the most common glycerolipids and sphingolipids. The spots contain 100 pmol of lipid (*A*). A commercial membrane was used in *B*, with lipids as specified by the producer. The first spot contains 100 pmol of lipid, followed by five successive 2-fold serial dilutions. cer, ceramide; glu-cer, glucosylceramide; gal-cer, galactosylceramide; lac-cer, lactosylceramide. *C*, binding of lipid analogues by protein as measured by surface plasmon resonance. The wild-type EqtII or mutants were immobilized on a surface of a CM5 sensor chip. The buffer used was 20 mM NaH_2PO_4, 140 mM NaCl, pH 7.0. The *curves* from *bottom* to *top* are for each analogue (4–16 μM) in increments of 2 μM. The *curves* were normalized to show the binding to 4000 RU of immobilized protein. The flow rate was 40 μl/min.

desired initial surface pressure. The final protein concentration in the well was 1 μM. The increment in surface pressure *versus* time was monitored until a stable signal was obtained.

Dot-blot Assay—Lipids were spotted on a charge-modified nylon membrane (Sigma) from a 100 pmol/μl stock solution in chloroform:methanol 4:0.1 (v/v). Sphingo Array, a commercial membrane spotted with lipids as specified by the producer (Product No. S-600C, Echelon), was also used. Membranes were first blocked for 4 h in 4% (w/v) bovine serum albumin (BSA) dissolved in 10 mM Tris-HCl, 150 mM NaCl, pH 8.0. Histidine-tagged protein at final 2.5 μg/ml concentration was then added, and the membrane was incubated overnight at room temperature on a rotary shaker. Membranes were washed three times (each time for 10 min) in 1% BSA. They were then incubated with mouse anti-polyhistidine antibodies in 1% BSA for 2 h, washed with 1% BSA as described above, incubated with secondary goat anti-mouse antibodies conjugated with horseradish peroxidase, and finally washed with 1% BSA as above. The dot-blot was developed by using 4-chloro-1-naphthol as a substrate.

ThermoFluor Assay—To test the thermal stability of the EqtII fold in the presence and absence of lipid analogues we used the ThermoFluor approach (36). Temperature scans from 4–100 °C were performed with 5 μg of EqtII alone and in the presence of phosphocholine (concentrations up to 1 mM) and acetyl-SM (concentrations up to 28 μM) while monitoring the fluorescence of the dye SYPRO Orange (Molecular Probes). The fluorescence of SYPRO Orange increases upon unfolding of the protein, and hence reports on changes in protein fold and stability are made possible.

Molecular Modeling and Calculation of the Electrostatic Properties—The structure of cytolysin from *Sagartia rosea* was modeled using SWISS-MODEL (37). The electrostatic properties were calculated and visualized with GRASP as described previously (38). Structural figures were prepared with PyMol (39).

RESULTS

EqtII Directly Binds SM or SM Analogue but Not Other Lipids—We first examined whether EqtII employs SM or other lipids as a membrane receptor. We first performed a lipid dot-blot assay with a range of sphingolipids and some other lipids that were used in this study (Fig. 1*A*). EqtII recognized only two different sphingomyelins, *i.e.* from bovine brain and chicken egg (Fig. 1*A*). These two differ in the properties of the fatty acid acyl chain but possess the same headgroup. EqtII bound to SM in a concentration-dependent manner (Fig. 1*B*). EqtII did not bind to any other lipid tested, most notably cholesterol, phosphatidylcholine, and any of the other sphingolipids used, *i.e.* ceramide, glucosylceramide, galactosylceramide, and monosialoganglioside G_{M1} (Fig. 1, *A* and *B*). It also did not bind other sphingolipids and glycerol-based phospholipids not presented in Fig. 1, *A* and *B*, *i.e.* sphingosine, disialoganglioside (G_{D3}), 3-sulfogalactosylceramide, phosphatidic acid, phosphatidylethanolamine, phosphatidylinositol and some of its phosphorylated variants, lysophosphocholine, and lysophosphatidic acid. SPR analysis of chip-immobilized EqtII showed that the toxin could not bind phosphocholine, the headgroup of PC and SM, or other PC analogues, *i.e.* dipropionoylphosphatidylcholine and lysophosphatidylcholine. However, it bound the water-soluble, short-chain SM analogue Ac-SM at μM concentrations (Fig. 1*C*). In summary, Fig. 1 shows that EqtII has the ability to directly and specifically bind to SM and the available water-soluble SM analogue, Ac-SM, in solution.

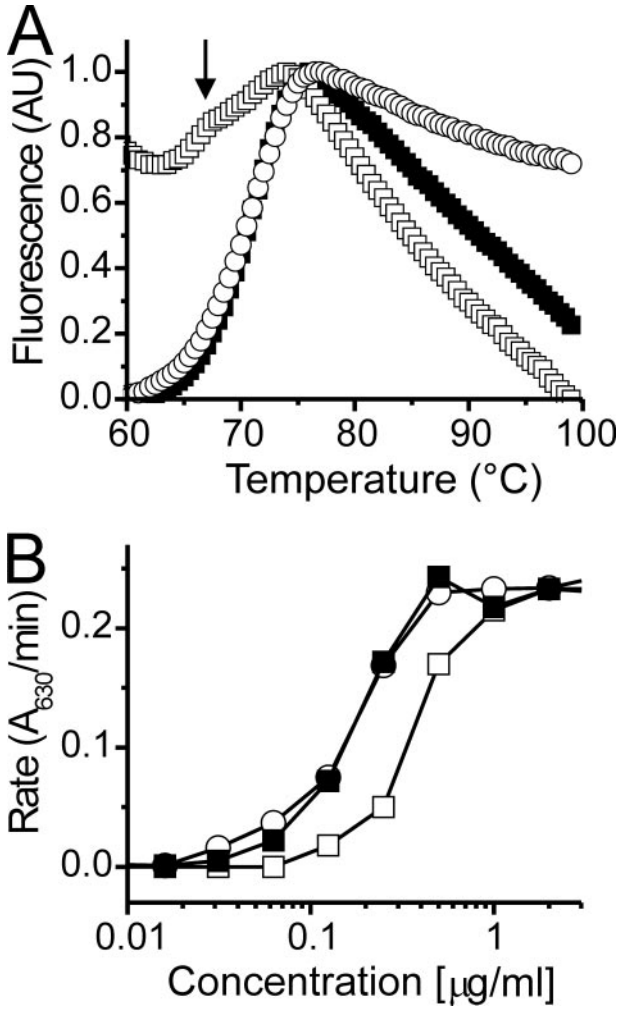

FIGURE 2. Conformational stability and inhibition of EqtII hemolysis in the presence of lipid analogues. *A*, thermograms of EqtII alone (*filled squares*) and in the presence of phosphocholine (*open circles*) and Ac-SM (*open squares*). The *arrow* indicates the pretransition unfolding peak observed in the presence of Ac-SM. *AU*, arbitrary units. *B*, hemolysis of bovine red blood cells was measured in the presence of lipid analogues at room temperature in 130 mM NaCl, 20 mM Tris-HCl, pH 7.4, by using a microplate reader. Hemolysis was monitored at 630 nm for 20 min at room temperature. *Filled squares*, no inhibitor; *open squares*, the presence of 5 μM Ac-SM; *open circles*, the presence of 3 mM 1,2-dipropionoyl-*sn*-glycero-3-phosphocholine.

The interaction of EqtII with phosphocholine and Ac-SM was also assessed with a thermal stability assay. Fig. 2*A* shows the fluorescence thermograms for EqtII alone and in the presence of phosphocholine and Ac-SM. As evident from the superposed thermal scans, phosphocholine does not influence the melting behavior of EqtII (peak at 76.0 °C for the EqtII alone and at 76.1 for EqtII in the presence of phosphocholine). However, Ac-SM changes the stability profile of EqtII markedly. In addition to the main transition, which shifts to a slightly lower temperature (peak at 73.8 °C), a pretransition peak can be

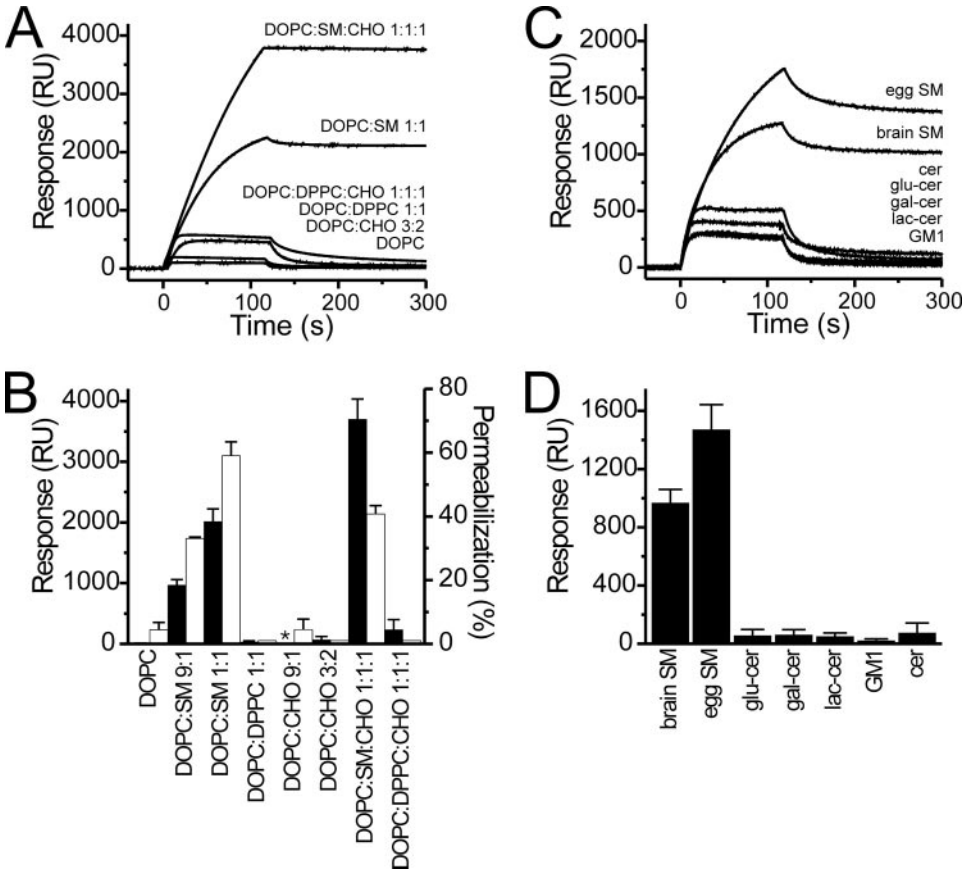

FIGURE 3. **The presence of SM in liposomes enables binding and permeabilization.** *A*, binding of EqtII to liposomes immobilized on the surface of L1 chip to ~10000 RU. The flow rate was 5 μl/min; the running buffer was 140 mM NaCl, 20 mM Tris-HCl, 1 mM EDTA, pH 8.5. The concentration of EqtII was 500 nM. *B*, the release of calcein from LUV of various lipid compositions (*open columns*) was measured at a lipid/toxin molar ratio 200. The concentration of lipids in vesicles buffer at 25 °C was 25 μM. The permeabilization induced by EqtII was expressed as the percentage of maximal permeabilization obtained at the end of the assay by the addition of detergent Triton X-100 to a final concentration of 2 mM. $n = 3–6$, average ± S.D. The amount of stably bound EqtII after 4 min of dissociation is shown for the comparison by *solid columns*. *, not measured. $n = 3–5$, average ± S.D. *C*, binding of EqtII to DOPC liposomes, which contained 10% (mol) of designated sphingolipids. The experimental conditions were as in *A*. *D*, the amount of stably bound EqtII after 4 min of dissociation. $n = 4$, average ± S.D.

observed (peak at 67.6 °C, *arrow* in Fig. 2*A*). The stability and hence the compactness of the EqtII structure is clearly reduced in the presence of Ac-SM compared with controls. Notably, the bimodal melting profile is indicative of a conformational change of EqtII upon Ac-SM binding, which phosphocholine alone is not able to induce. We further checked whether the presence of Ac-SM is able to inhibit EqtII-induced hemolysis of erythrocytes. Ac-SM was inhibitory at μM concentration, whereas neither dipropionoylphosphatidylcholine nor phosphocholine was inhibitory at mM concentrations (Fig. 2*B*). All of these data clearly show that EqtII can directly and specifically bind SM or its analogues but not PC, PC analogues, or cholesterol. Some previous studies have used many different lipids to assess the interaction with EqtII or sticholysin by measuring the inhibition of permeabilizing activity. Among lipids used in our binding assays, these studies also employed some other sphingolipids such as cerebrosides (25, 40, 41). They showed that only SM was able to considerably inhibit permeabilizing activity. Thus our direct binding studies are in excellent agreement with previous inhibitory tests.

Next we examined the role of SM in the binding of EqtII to liposomes. We tested the binding of EqtII to membranes using SPR by immobilizing liposomes of different composition on an L1 sensor chip. The binding of EqtII was negligible for DOPC and DOPC:cholesterol (3:2) liposomes but high and stable when liposomes composed of DOPC:SM (1:1) were used (Fig. 3*A*). These differences in binding might arise from SM-induced changes in the bilayer physical properties, *i.e.* changes in membrane bilayer fluidity, as SM has very different physical properties than DOPC. Hence we replaced SM with DPPC, a PC with disaturated acyl chains and physical properties similar to those of SM and the ability to induce lipid domain formation in binary and ternary mixtures (42, 43). Although the binding of EqtII to DOPC:DPPC (1:1) membranes was slightly better in the association phase than for DOPC membranes, it was reversible, and the final amount of stably bound protein was negligible in comparison with DOPC:SM (1:1) liposomes (Fig. 3). We have also checked binding to DOPC:SM:cholesterol (1:1:1), a ternary lipid mixture that should allow the formation of lipid domains (42, 43). The binding to these membranes was stable and irreversible, but replacing SM with DPPC again reduced binding dramatically. These binding results are in agreement with permeabilizing assays in which EqtII could readily permeabilize liposomes that contained only a minor amount of SM (10 mol %, Fig. 3*B*). Concentrations as high as 40 mol % cholesterol did not even lead to a modest increase in permeabilization activity. Neither DPPC included in DOPC liposomes nor a ternary mixture of DOPC:DPPC:cholesterol (1:1:1) was sensitive to toxin action. We further checked how the presence of different sphingolipids affects binding. We used DOPC liposomes that contain 10% (mol) of various sphingolipids. As expected, the binding to either porcine brain or chicken egg SM was significant and irreversible, whereas it was negligible for all other sphingolipids tested (Fig. 3, *C* and *D*).

Finally, we examined how the composition of red blood cell membranes affects the binding and hemolytic activity of EqtII. The removal of accessible SM from human erythrocyte membranes by sphingomyelinase (Fig. 4*A*) protected them against toxin action (Fig. 4*B*), as reported for sticholysin (25). The removal of up to 80% of cholesterol from the lipid membranes had no effect on the hemolytic activity (Fig. 4*B*). We tested

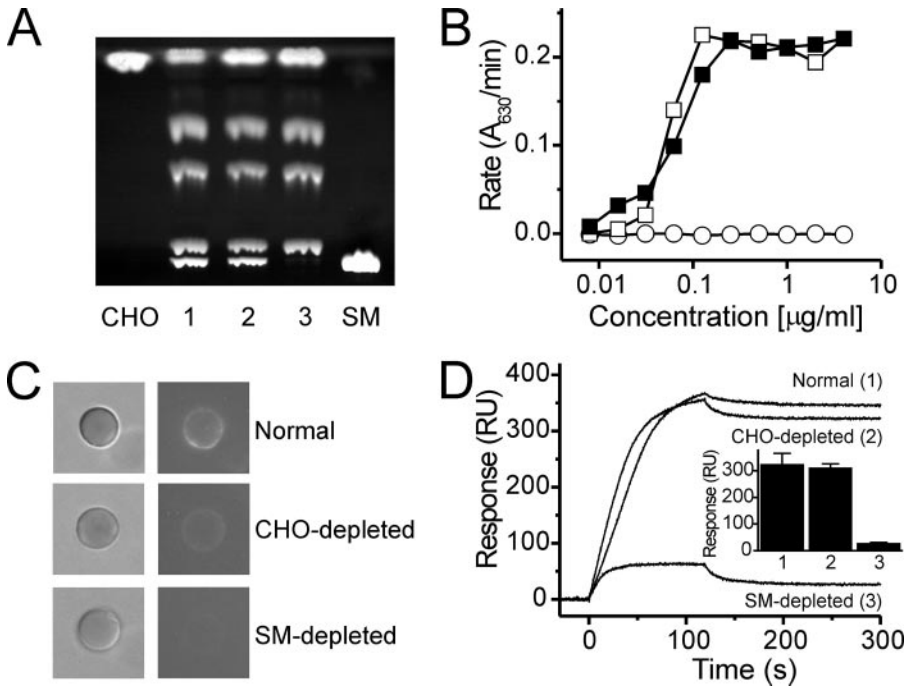

FIGURE 4. **Removal of SM protects human erythrocytes against permeabilizing activity of EqtII.** *A*, thin layer chromatography of lipid extracts from red blood cells used in this experiment. *Lane 1*, cholesterol (*CHO*)-depleted erythrocytes; *lane 2*, normal erythrocytes; *lane 3*, SM-depleted erythrocytes. The position of cholesterol or SM standards is denoted at the side of the image. *B*, hemolysis of human red blood cells was measured exactly as explained in the legend for Fig. 1. *Filled squares*, untreated erythrocytes; *open circles*, SM-depleted erythrocytes; *open squares*, cholesterol-depleted erythrocytes. *C*, binding of NBD-labeled EqtII G27C mutant to erythrocytes prepared as in *A*. *Left panel*, erythrocyte under bright field microscope; *right panel*, NBD fluorescence of the same erythrocyte. *D*, binding of EqtII to erythrocyte ghosts, prepared from erythrocytes as in *A* and monitored by SPR. A typical trace is shown from four binding experiments. Erythrocyte ghosts were immobilized on an L1 chip (Biacore AB) to a final value of ~1200 RU. The flow rate was 20 μl/min. The concentration of EqtII was 50 nM. The *inset plot* summarizes the amount of stably bound EqtII at the end of the dissociation phase, *i.e.* after 3 min of dissociation. *Column 1*, ghosts from untreated erythrocytes (labeled *Normal* in the *left panel*); *column 2*, ghosts from cholesterol-depleted erythrocytes; *column 3*, ghosts from SM-depleted ghosts. $n = 4$, average ± S.D.

whether this lack of hemolytic activity was due to a reduced binding to erythrocyte membranes. An NBD-labeled G27C mutant of EqtII (16) stained normal and cholesterol-depleted erythrocytes but not membranes of SM-depleted erythrocytes (Fig. 4*C*). Similarly, we could only detect poor and reversible binding to SM-depleted erythrocyte ghost membranes in SPR experiments. In contrast, untreated and cholesterol-depleted ghost membranes bound EqtII in an irreversible manner (Fig. 4*D*).

In summary, EqtII is clearly able to bind SM directly and specifically. The presence of this lipid in membranes significantly improves permeabilizing and hemolytic activities. These effects are clearly not due to changes in the physical properties of SM-containing membranes, as DPPC with similar physical properties did not enable binding nor permeabilizing activity.

Properties of the Actinoporin Membrane Binding Site—The first contact of actinoporins with the membrane is mediated by exposed amino acid residues on one side of the molecule (20, 21). This interfacial binding site (IBS) is composed of aromatic residues, in particular an exposed tryptophan at position 112, and the POC binding site. According to the crystal structure of StII, the POC binding site is composed of Ser^{54}, Val^{87}, Ser^{105}, Pro^{107}, Tyr^{133}, Tyr^{137}, and Tyr^{138} (15). These residues are almost completely conserved in the actinoporin family (Fig. 5*A*), indicating that phosphocholine binding may proceed in the same way in all actinoporins. However, Trp^{112} is not well conserved, being replaced by Phe or Leu in other actinoporins (Fig. 5).

Although most members of this extremely conserved family of proteins are basic proteins with an isoelectric point above pH 9, one member, a cytolysin from *S. rosea*, is acidic and has a pI of ~5 (44). All described members, including *S. rosea* cytolysin, display sphingomyelin-specific enhancement of pore-forming activity (45–47). Even though the three-dimensional structure of these proteins is very similar (13–15), the charge distribution varies widely among different members of actinoporins (Fig. 5*C*). Specifically EqtII, with a net charge of +6, possesses two prominent regions of positive charge: one around loops at the bottom of the molecule and around the C-terminal helix and the other around loops at the top of the molecule. Despite a net charge of +3, there is no particular regional accumulation of charge in StII (Fig. 5*C*). This may explain why StII was found to be a tetramer in solution (48), whereas EqtII is monomeric (45). *S. rosea* cytolysin, with a net charge of −4, has an evenly distributed negative charge on the front of the β-sandwich (Fig. 5*C*). Obviously, actinoporins do not share similar bulk electrostatic properties. One common feature, however, is the absence of charge around the IBS (Fig. 5*C*). This might imply that membrane interactions are largely hydrophobic in nature and that electrostatic interactions play only a minor role in binding. The properties of the IBS led us to explore the structural basis for the discrimination between SM and PC by studying the effects of site-directed mutagenesis at functional positions within the IBS of EqtII.

Role of Trp^{112} in Membrane Binding and Sphingomyelin Recognition—Because PC and SM have the same phosphorylcholine headgroup, the toxin needs to recognize SM elsewhere. Trp^{112} was recognized as one of the most important residues for the membrane binding of EqtII (20, 21) (Fig. 5*B*). To test for the role of this exposed residue in the specific recognition of SM, we replaced tryptophan by alanine (W112A) and also checked whether a natural variant from *Phyllodiscus semoni* (W112L, Fig. 5*B*) possesses the same SM-specific properties as the wild-type EqtII. To test the influence of electrostatic properties of the IBS in the membrane-binding step, Trp^{112} was mutated to glutamic acid (W112E), introducing a negative charge, or to arginine (W112R) to introduce a positive charge.

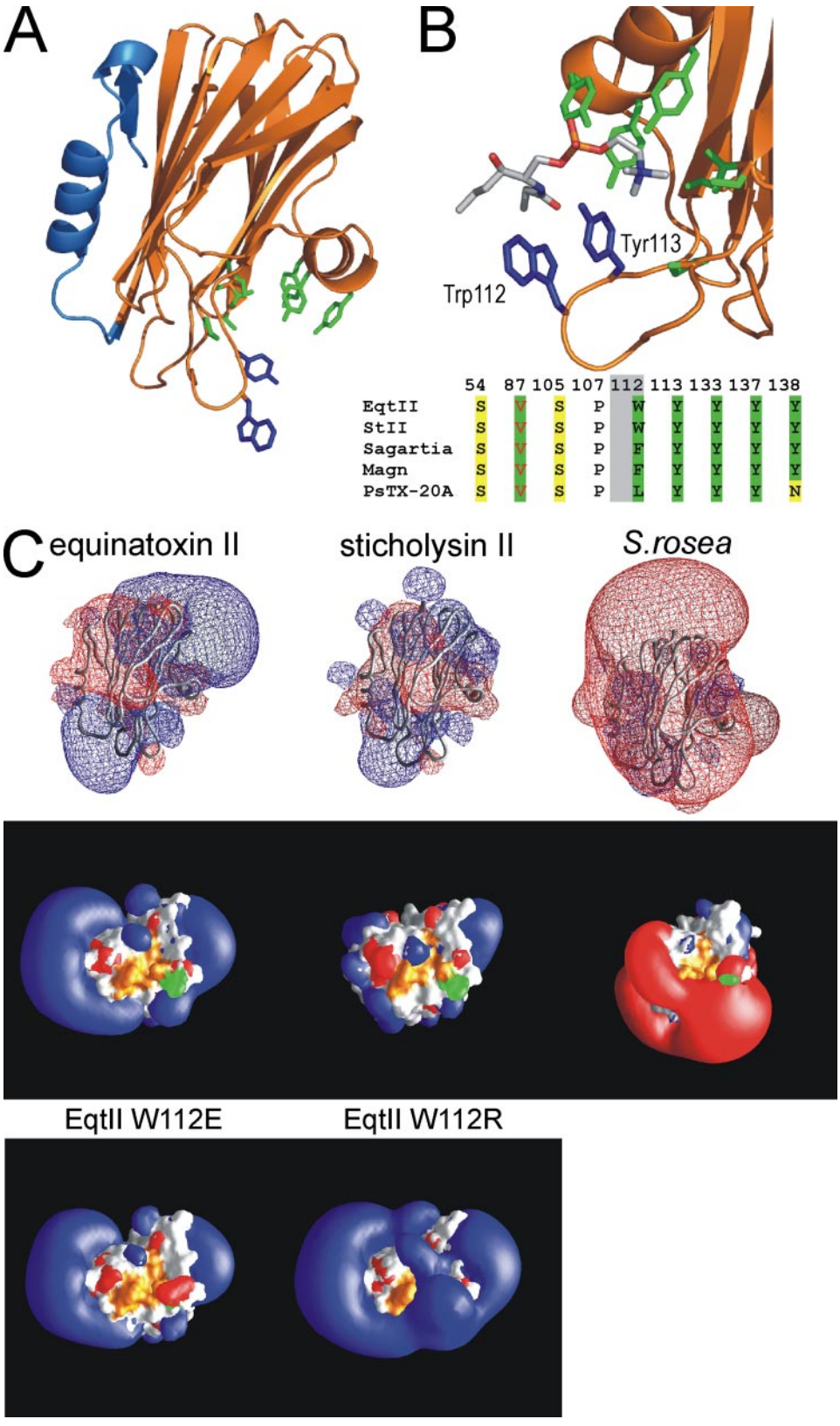

FIGURE 5. **Properties of actinoporin structures.** *A*, three-dimensional structure of EqtII. The N-terminal region that participates in the membrane interactions and form the walls of the conductive channel is labeled in *blue*. The residues that participate in POC binding are labeled in *green* and denoted by *sticks*. Trp^{112} and Tyr^{113} are shown in *blue*. *B*, the model of SM bound to EqtII based on a crystal structure of a closely related sticholysin II complexed with phosphocholine (15). Side chains that participate in POC binding are represented as *sticks* and are shown in the alignment *below* for some of the actinoporins. Trp^{112} and Tyr^{113} are shown in *blue*. The exposed Trp^{112}, not part of phosphocholine binding site, is shaded *gray* in the alignment. Only selected carbon atoms of sphingosine and fatty acid of SM are shown. *C*, The charge distribution in related actinoporins. The orientation of the molecule is the same as shown in *A*. The *middle row* shows the bottom of the molecule, *i.e.* the molecule in *A* as viewed from below. The residues that participate in POC binding are labeled in *orange*, and the exposed residue at position 112 is shown in *green*. The *red* color represents negative charge isopotential, and the *blue* represents the positive charge.

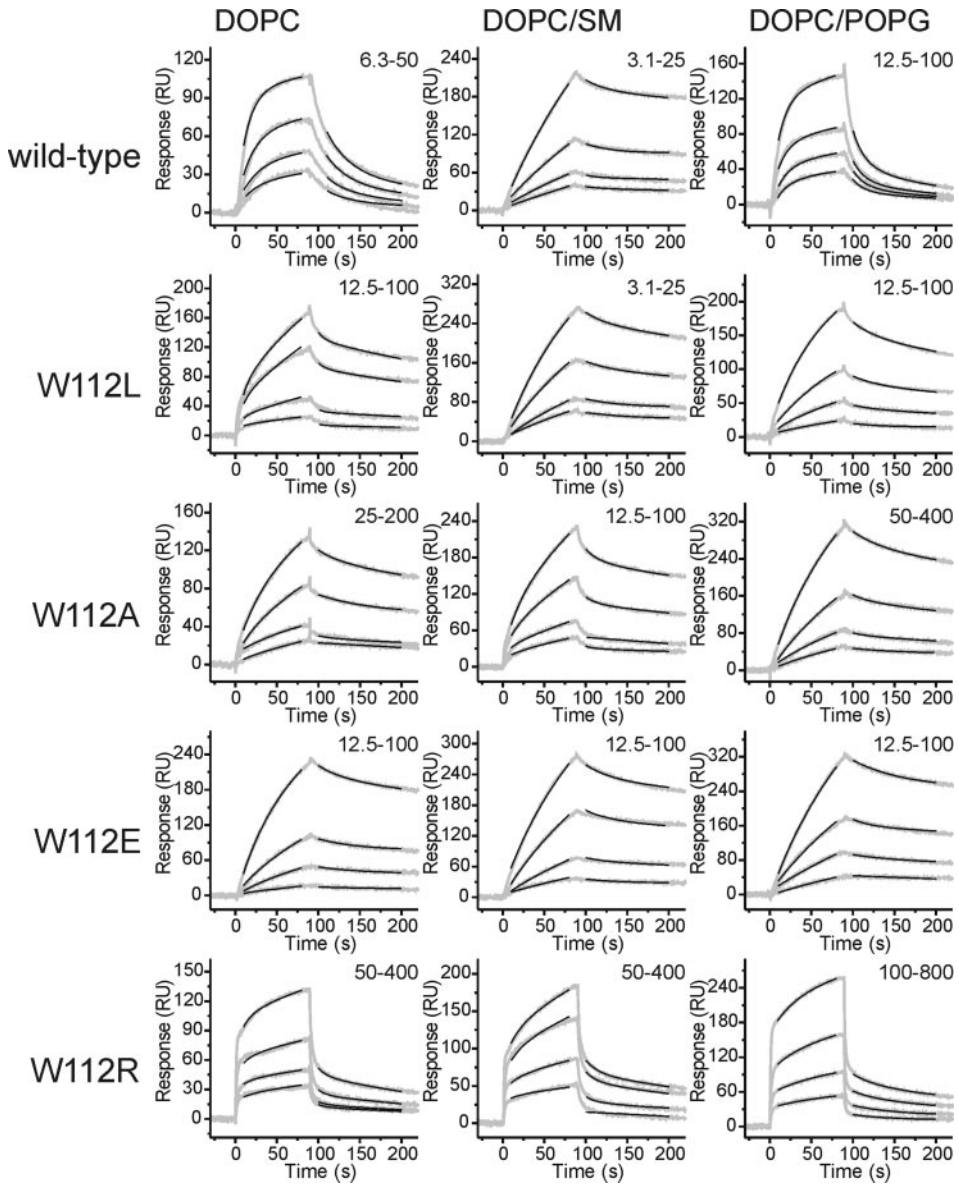

FIGURE 6. **Binding of EqtII and Trp^{112} mutants to liposomes.** Shown is the binding of EqtII and Trp^{112} mutants to liposomes immobilized on the surface of L1 chip to ~10000 RU. The flow rate was 30 μl/min, and the running buffer was 140 mM NaCl, 20 mM Tris-HCl, 1 mM EDTA, pH 8.0. For each protein at each membrane four different concentrations, in 2-fold increments, were used. The concentrations (nM) are denoted in the *right-hand corner* of each panel. The experimental data were globally fitted to a two-step kinetic model. The derived kinetic constants are reported in Table 1 and supplemental material.

The overall charge around the IBS was diminished in the mutant W112E (Fig. 5*C*), whereas in W112R, the IBS was almost completely covered with positive charge. The electrostatic properties of W112L and W112A remained unchanged. We used these mutants to perform a detailed kinetic analysis of liposome binding, insertion into lipid monolayers, and permeabilization assays.

The binding of each mutant to liposomes of different lipid composition was tested by SPR (Fig. 6). Sensorgrams exhibit complex binding kinetics and could not be analyzed by a 1:1 binding model, in agreement with a multi-step pore-forming mechanism of actinoporins (21, 45, 46). However, we were able to analyze the data by fitting the sensorgrams to a two-step binding model, described previously in Hong *et al.* (21) (Table 1 and supplemental material). The first step represents the initial association of the toxin with the membrane and the second step corresponds to the transfer of the N-terminal region to the lipid membrane. The binding of the wild type to DOPC and to DOPC:POPG (1:1) liposomes was reversible. Use of SM (DOPC:SM (1:1) liposomes) drastically reduced the desorption from the bilayer surface, and the equilibrium dissociation constant (K_D) increased almost 10-fold from 6 to 57 nM (Table 1). W112L behaved similarly to the wild type and bound best to DOPC:SM (1:1) liposomes (K_D = 9 nM) as compared with DOPC liposomes (K_D = 48 nM). However, this mutant had a slightly better membrane association with DOPC and DOPC:POPG (1:1) membranes than the wild-type EqtII. W112A and W112E mutants bound similarly to all three different membrane types, and K_D values did not vary much. Notably, mutant W112R bound to liposomes only at much higher concentrations, and the binding was reversible for all membrane compositions. Equilibrium dissociation constants were up to 2 orders of magnitude larger than the ones of the wild type (Table 1).

We next examined the ability of proteins to insert into lipid monolayers of the same lipid compositions used for SPR experiments. The increase in the lateral pressure was followed after addition of the protein to the subphase (Fig. 7, *left column*). We checked several different initial pressures, and from the final

TABLE 1

Summary of SPR and lipid monolayer results

The equilibrium dissociation constants derived from the fits (see also supplemental material) of sensorgrams presented in Fig. 6 are shown to the left, and critical pressures of lipid monolayer insertion derived from the plots in Fig. 7 are shown to the right for each lipid composition tested.

Protein	DOPC		DOPC:SM (1:1)		DOPC:POPG (1:1)	
	$K_D \times 10^{-8}$	π_c	$K_D \times 10^{-8}$	π_c	$K_D \times 10^{-8}$	π_c
	M	mN/m	M	mN/m	M	mN/m
EqtII	5.7	31.0	0.6	36.5	26.8	29.9
W112L	4.8	27.9	0.9	36.4	4.2	36.4
W112A	4.1	27.5	6.2	32.4	12.6	36.1
W112E	1.4	28.2	2.3	25.5	2.2	34.4
W112R	51	19.1	141	24.9	51	26.2

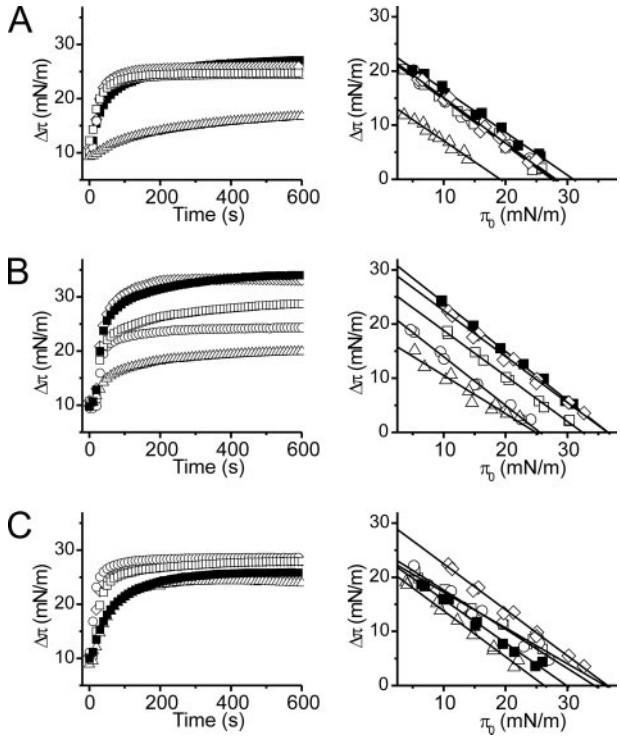

FIGURE 7. **Insertion of EqtII and Trp^{112} mutants in lipid monolayers.** An increase in the surface pressure after insertion of EqtII and mutants in lipid monolayers was followed until stable signal was achieved. The aqueous subphase was composed of 500 μl of 10 mM Hepes, 200 mM NaCl, pH 7.5. The final protein concentration in the well was 1 μM. The *black lines* on the *right panels* are linear fits of the experimental data. The critical pressures, *i.e.* pressures at which no insertion can occur, were calculated from the fits and are reported in Table 1. *Solid squares*, wild-type EqtII; *open diamonds*, W112L; *open squares*, W112A; *open circles*, W112E; *open triangles*, W112R. Lipid monolayers tested were from DOPC (*A*), DOPC:SM (*B*), and DOPC:POPG 1:1 (*C*).

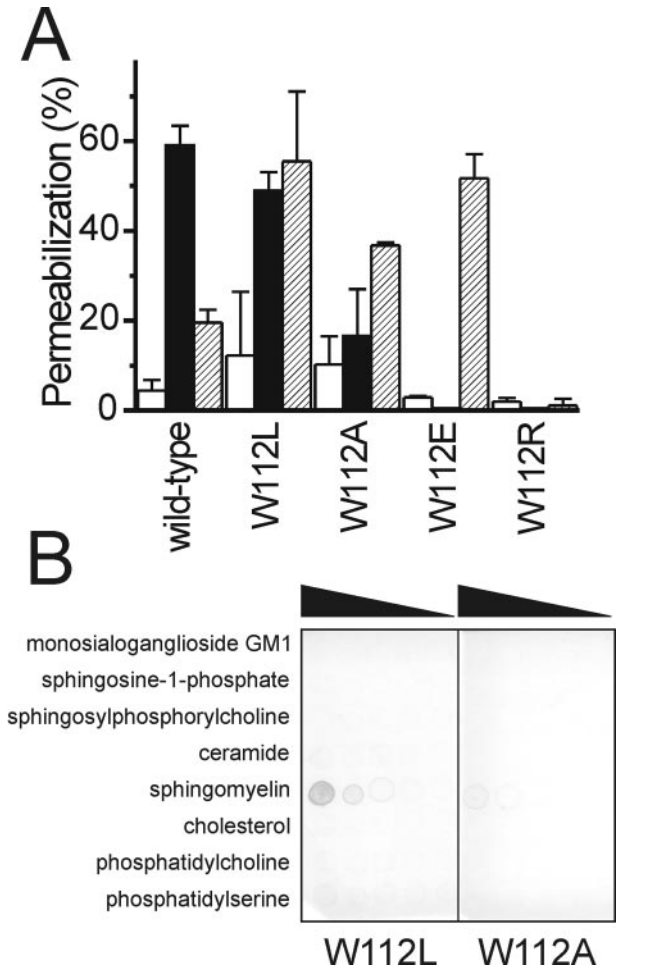

FIGURE 8. **Calcein release and direct binding of SM by Trp^{112} mutants.** *A*, calcein release from liposomes. The experiments were performed as described in the legend for Fig. 3. *White columns*, DOPC liposomes; *black columns*, DOPC:SM 1:1 liposomes; *hatched columns*, DOPC:POPG (1:1) liposomes. n = 2–6, average ± S.D. The data for the wild-type EqtII for DOPC and DOPC:SM from Fig. 3 are shown again for the comparison. *B*, dot-blot binding assay. The first spot contains 100 pmol of lipid followed by five successive 2-fold serial dilutions.

increases we constructed critical pressure plots (Fig. 7, *right column*). From a linear fit we obtained the critical insertion pressure for each lipid composition, π_c, *i.e.* the initial pressure at which no further insertion of proteins could be achieved (Table 1). All proteins except W112R inserted into DOPC monolayers to a similar degree (Fig. 7), with critical pressures ranging from 28.2 to 31 mN/m. Insertion was better for the DOPC:SM (1:1) mixture, particularly for the wild type and W112L, which had critical pressures of 36.5 and 36.4 mN/m, respectively. The insertion of W112A into SM-containing monolayers was slightly better than into DOPC monolayers, but π_c, at 32.4 mN/m, was still significantly lower than for W112L and the wild type. The insertion into DOPC:POPG (1:1) monolayers was strong for W112L, W112A and W112E, which all yielded a similar π_c, around 36 mN/m. However, the wild type EqtII incorporated into these and DOPC monolayers to a similar extent. W112R inserted much less than other mutants, having the lowest π_c of all proteins tested for each lipid composition.

SPR and monolayer experiments were in good agreement with permeabilization studies. Permeabilizing activity of W112L was similar to that of the wild-type and significantly increased when SM was present in the liposomes (Fig. 8*A*). In contrast to the wild type, W112L released calcein to the same extent from POPG- and SM-containing liposomes. In comparison, the release by the wild type from DOPC:POPG (1:1) liposomes was only 19.6 ± 2.8% (average of two experiments ± S.D.). The permeabilizing activities of W112A and W112E were below 20% for DOPC and DOPC:SM (1:1) liposomes but around 40% in DOPC:POPG (1:1) liposomes. W112R did not release calcein from any of the liposomes tested.

In Fig. 8*B* we also examined the direct binding of mutants W112L and W112A to various lipid species. A dot-blot assay showed that W112L could bind SM, whereas W112A could not. Moreover, W112A exhibited a much weaker binding of Ac-SM in an SPR assay compared with the wild type (Fig. 1*C*).

The results show that the natural variant W112L possesses wild-type lipid specificity. In addition, this mutant also showed better association, insertion, and permeabilizing activity in membranes or monolayers composed of DOPC:POPG. The removal of the leucine or indole side chain resulted in a loss of sphingomyelin specificity, as apparent from the properties of mutant W112A. Finally, charge does not seem to play an important role in binding, as neither negatively charged lipid nor charge manipulation of the IBS could alter the binding properties of the proteins.

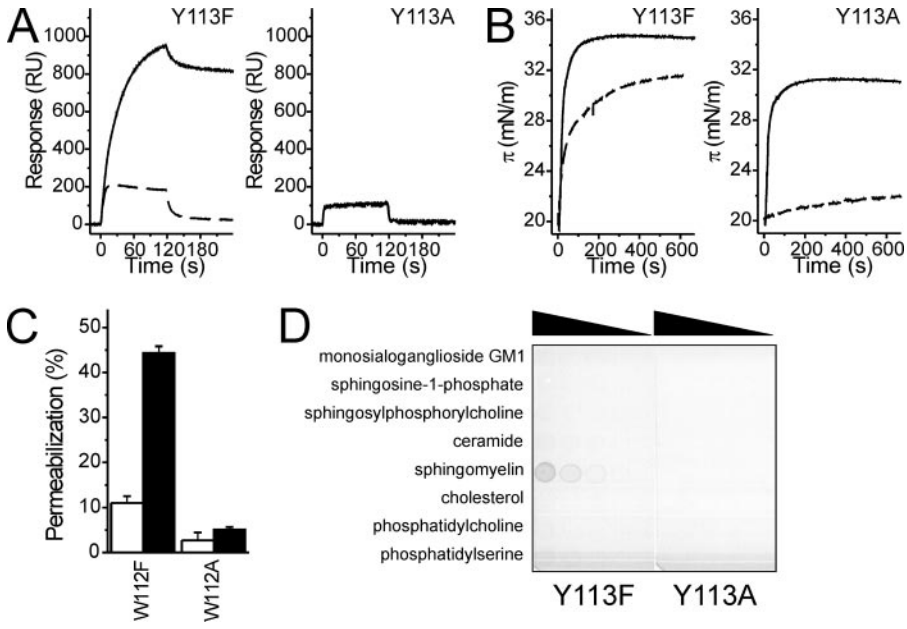

FIGURE 9. **Properties of Y113F and Y113A mutants.** *A*, binding to DOPC (*dashed line*) or DOPC:SM (*solid line*) liposomes. The experiment was performed as explained in the legend for Fig. 4. *B*, insertion in lipid monolayers composed of DOPC (*dashed line*) or DOPC:SM (*solid line*). The experiment was performed as explained in the legend for Fig. 7. *C*, calcein release. *Open columns*, DOPC; *filled columns*, DOPC:SM. *D*, dot-blot binding assay. The first spot contains 100 pmol of lipid followed by five successive 2-fold serial dilutions.

Role of Tyr^{113} in SM Binding—Another residue that is close to the SM headgroup and could affect SM specificity is Tyr^{113} (Fig. 5*B*). To test for potential hydrogen bond formation between the Tyr^{113} hydroxyl group and the characteristic amide on SM, we generated mutant Y113F. Mutant Y113A was used to examine the importance of the aromatic ring at this position. Mutant Y113F behaved similarly to the wild type in all of the tests we performed. In an SPR assay it bound to the DOPC:SM liposomes to a much higher degree than to DOPC liposomes (Fig. 9*A*). It showed preference for SM when used in lipid monolayer assays (Fig. 9*B*) and could release calcein from the DOPC:SM liposomes but not from the DOPC liposomes (Fig. 9*C*). It also bound SM in dot-blot assay but did not bind any of the other lipids tested (Fig. 9*D*). In contrast, mutant Y113A failed to show an increased activity in the presence of SM in all of the above described assays (Fig. 9). It did not recognize SM directly (Fig. 9*D*) and showed poor binding to Ac-SM (Fig. 1*C*). Mutants Y113A and W112A thus behaved similarly, indicating that not only the Trp^{112} residue is needed for specific recognition of SM but also the aromatic ring of Tyr^{113}.

DISCUSSION

In this paper we show that EqtII specifically employs SM as its membrane receptor and that Trp^{112} and Tyr^{113} are crucial for this specificity. Membrane binding of actinoporins is not yet understood at the molecular level, and it was believed for a long time that SM was the receptor for actinoporins in lipid membranes. This view was challenged by recent reports showing that membranes without this lipid are also sensitive to these toxins (26–28). StII, for instance, has been shown to permeabilize cholesterol-containing PC membranes (26), and coexistence of different lipid phases is advocated to be important for the EqtII action (28). Recently, it has also been shown that StII binds to cell membranes via lipid rafts (49). Similar to our results (*cf.* Fig. 3); however, cholesterol-containing or phase-separated membranes without SM had only modest effects compared with membranes that contain SM. When discussing the role of particular lipids in toxin action, it is important to distinguish between direct interaction of protein toxin with a certain lipid, which usually enables specific attachment of the toxin to particular membranes, and effects that originate from the physical properties of the membrane when particular lipid mixtures are used. It is therefore highly likely that the observed increased permeabilizing potency of actinoporins against PC liposomes in the presence of cholesterol is due to cholesterol-induced membrane microdomain formation and, hence, to the enhanced accessibility of the phosphorylcholine group. A recently proposed model of EqtII binding to the borders between gel-fluid or liquid ordered-disordered domains is in agreement with this proposition, as the lipid packing defects between the two domains might better expose phosphorylcholine headgroups for binding of EqtII and enhance transfer of the N-terminal α-helix across the lipid bilayer (28).

In this report we aimed to address whether EqtII could directly bind to and specifically recognize SM (25). This has a direct and important biological significance, as lipid recognition is important for targeting of toxin to prey membranes and, at the same time prevents self-damage, because the toxin is not active against membranes of sea anemones, which contain an SM analogue (50). To address this question, we used various functional assays to test the direct binding of EqtII to SM (Fig. 1). In dot-blot assays we showed that EqtII possesses an exclusive SM binding capacity. In addition, SPR experiments proved that binding of a SM analogue is clearly due to the presence of unique amido or hydroxyl groups on SM, in agreement with the notion that EqtII needs to discriminate between PC and SM below the headgroup region. We also found that hydrophobic interactions between the SM tail and hydrophobic patches of EqtII are not likely to contribute to SM specificity. Lysophosphatidylcholine has a similar chain length as the SM analogue Ac-SM but, in contrast, could not specifically bind to EqtII (Fig. 1*C*).

The two most important residues for the binding and recognition of a single SM molecule are Trp^{112} and Tyr^{113}, located on a broad, exposed loop within hydrogen-bonding distance of the distinctive hydroxyl and amide groups of the SM ceramide moiety. All other amino acids are too distant to participate directly in SM recognition (Fig. 5). When side chains of Trp^{112} and Tyr^{113} were mutated to alanine, a large decrease in permeabi-

lizing activity, binding to immobilized liposomes, and insertion into lipid monolayers was observed (Figs. 6–9). Furthermore, the direct binding of these mutants to SM and Ac-SM was reduced (Figs. 1, 8, and 9). In contrast, the W112L and Y113F mutants exhibited similar SM specificity, although the activity in all *in vitro* tests was always lower than for the wild-type protein (Figs. 6–9). The hydroxyl group of Tyr^{113} is not important for specificity, as Y113F displayed similar activity in all of our SM recognition tests. Therefore, other interactions requiring the aromatic ring are likely, *e.g.* π electron aromatic residue-SM amide interactions (51). The exposed residue at position 112 not only provides the free energy for interaction with the membrane (21, 27, 52) but also stabilizes bound SM by hydrophobic interactions, as leucine was equally acceptable. Exposed tryptophans of membrane proteins or model α-helical peptides are generally located within the lipid-water interface (53–55). The indole rings of tryptophans are buried in the acyl chain region of the membrane, and the NH groups are located in the lipid-water interphase, as shown in a recent computational analysis of peripheral proteins (56). Trp^{112} is perfectly suited for these tasks, as it is within hydrogen-bonding distance of SM (Fig. 5) and contributes both to SM recognition and stabilization of membrane-bound EqtII.

SPR experiments enabled us to perform a direct kinetic analysis of the role of Trp^{112} in the membrane binding of EqtII. EqtII bound stably and with a low dissociation constant to SM-containing membranes, either LUVs or erythrocyte ghost membranes (Figs. 3*A*, 4*C*, and 6). This mode of binding may be a general feature of pore-forming toxins, *i.e.* irreversible binding to the membranes is achieved upon interaction with a specific lipid receptor but not when binding to other lipids, as shown for cholesterol-dependent cytolysins (57) and lysenin (58). Thus the membrane-binding step is distinctively different from that of other membrane binding domains, where a reversible binding was observed in many the studied examples (59–61). The equilibrium dissociation constant for the binding of EqtII to supported LUVs composed of DOPC:SM (1:1) (K_d = 6 nM) is comparable with that of the binding to tethered lipid bilayers composed of DOPC:SM (1:1) (K_d = 7.5 nM), which was also determined by SPR (21), thus supporting the chosen experimental system used for evaluating EqtII binding to membranes. When comparing the binding of various mutants to liposomes composed of DOPC:SM (1:1), we observed the following trends in changes of kinetic parameters (Table 1 and supplemental material): the largest effects were observed in the first step of the binding, k_{d1}, changed 4- and 7-fold for W112A and W112R, respectively. Interestingly, k_{a1} was decreased for the mutants W112E and W112R, as obviously charge manipulation of the IBS affects association with the membrane and further points to the role of hydrophobic interactions in EqtII membrane association. Other parameters, particularly k_{a1} and k_{d2}, changed little. When comparing DOPC:SM (1:1) and DOPC membranes, a large increase in k_{d1} was observed only for the wild type and W112L, implying that specific protein-SM interactions slow down the dissociation from SM-containing membranes. In agreement with other functional data, W112A showed slightly better dissociation in the presence of SM. However, only in the case of the wild type did the presence of SM also change k_{a2} and k_{d2}, resulting in an almost 8-fold decrease in K_{d2}. These changes were not observed for the studied mutant, which additionally points to the specific interaction between Trp^{112} of the wild-type EqtII and SM.

Nonspecific electrostatic interactions mainly affect the association step of some peripheral protein domains involved in cell signaling, *i.e.* the Pleckstrin homology (PH) domains, Phox homology (PX) domains, and protein kinase C conserved-2 domains (C2) employ electrostatic attraction together with specific lipid binding to exhibit diverse affinity and specificity toward negatively charged lipids of internal cell membranes such as phosphoinositides or phosphatidylserine (62). These domains show a clearly conserved electrostatic pattern on the surface of the protein, where a strong positive potential is surrounding the hydrophobic lipid binding site (63, 64). EqtII shares this organization (Fig. 5*C*) with an abundance of positive charge around the IBS. It has already been proposed that this positive charge may help in the initial contact of EqtII with the membrane (65). However, this structural feature is not conserved among actinoporins, and it seems that electrostatic interactions are not important for the specific recognition of SM-containing membranes and other interactions are predominant. This was highlighted by SPR experiments on negatively charged membranes to which wild-type EqtII showed the worst binding of all tested proteins. This is in good agreement with the observation that high salt concentrations do not affect the binding of the toxin to SM-containing membranes (21). The wild type also inserted to a lesser extent into negatively charged monolayers, and the calcein release from liposomes composed of negatively charged lipids was reduced. All mutants except W112R, which could not permeabilize membranes under any condition, showed increased activity on negatively charged DOPC:POPG membranes. The mutations to other side chains thus reduced the influence of Trp^{112}, and in negatively charged membranes electrostatic interactions prevailed due to the positively charged belt around the IBS. In summary, if no SM is bound, *i.e.* in DOPC membranes for the wild type or W112L and in DOPC:SM 1:1 membranes for W112A, the binding is not stable and thus is short-lived, and the insertion and permeabilization will be low or nonexistent (Figs. 7 and 8). If SM is recognized via residues at positions 112 and 113, stable binding will occur, with subsequent insertion of the N-terminal region into the lipid membrane (21).

The described molecular mechanism of SM recognition puts some previously published data on actinoporins in a clearer structural context. The importance of tyrosyl side chains for toxin function was shown by Turk *et al.* (66), where chemical modification of tyrosines in EqtII almost completely abolished hemolytic activity. In agreement with our model, in sticholysin II a mutation of the tyrosine equivalent to Tyr^{113} (mutant Y111N) largely abolishes hemolytic activity (67). Furthermore, by introducing a ^{19}F label on EqtII tryptophans, it was shown that Trp^{112} is important for SM recognition, as specific NMR chemical shifts were observed upon the addition of SM to PC micelles (31). The preferential engagement of SM by the toxin was inferred also from solid-state NMR data (68). Finally, and most importantly, sea anemones are protected against the action of actinoporins by the absence of SM in their mem-

branes. Instead, they possess phosphonosphingolipids that have an altered phosphorylcholine headgroup (50).

SM-specific proteins are widespread in nature and are found in bacteria (69, 70), fungi (71), and animals, *i.e.* sea anemones (7) and earthworms (58). They are major virulence factors in bacteria and eukaryotic protein toxins, which use SM as a receptor to attach effectively to eukaryotic cell membrane rafts. There are, however, no high-resolution structural details of SM recognition available. Emerging studies indicate that aromatic amino acids are important for the interaction with membrane SM. Neutral sphingomyelinases, membrane-damaging virulence factors of Gram-positive bacteria, possess a β-hairpin with exposed aromatic residues that participate in the binding of membrane SM (69, 70). Tryptophans are also involved in SM binding of the earthworm pore-forming toxin, lysenin (72). In addition, a so-called "sphingolipid-binding motif" was discovered in the V3 loop of human immunodeficiency virus envelope glycoprotein gp120, an Alzheimer β-amyloid peptide, and human prion proteins. This motif is composed of a hairpin structure with one or two flanking α-helices. In all three cases the tip of the hairpin structure contains conserved aromatic residues responsible for lipid recognition (73). This motif is, however, not specific only to SM but is able also to bind other sphingolipids such as galactosylceramide. This is not the case for EqtII, as it interacts solely with SM of all the lipids tested, as shown here by us and by others in previous work (25, 40, 41). We conclude that the actinoporin phosphorylcholine binding site, with a bulky hydrophobic amino acid at position 112 and an aromatic ring at position 113, may represent a generic three-dimensional structural motif able to bind a single SM molecule either in solution or in a lipid bilayer.

Acknowledgments—We thank Dr. Aleš Kladnik for help with the fluorescence microscope, Prof. Robert Lightowlers for Biacore advice and support, Dr. Gregor Gunčar for help with the preparation of Fig. 5, and Vesna Hodnik for excellent technical assistance.

REFERENCES

1. Simons, K., and Ikonen, E. (1997) *Nature* **387,** 569–572
2. van Meer, G. (2005) *EMBO J.* **24,** 3159–3165
3. Manes, S., del Real, G., and Martinez, A. (2003) *Nat. Rev. Immunol.* **3,** 557–568
4. Lafont, F., Abrami, L., and van der Goot, F. G. (2004) *Curr. Opin. Microbiol.* **7,** 4–10
5. Kiyokawa, E., Baba, T., Otsuka, N., Makino, A., Ohno, S., and Kobayashi, T. (2005) *J. Biol. Chem.* **280,** 24072–24084
6. Hanada, K., Kumagai, K., Yasuda, S., Miura, Y., Kawano, M., Fukasawa, M., and Nishijima, M. (2003) *Nature* **426,** 803–809
7. Anderluh, G., and Maček, P. (2002) *Toxicon* **40,** 111–124
8. Anderluh, G., and Maček, P. (2003) in *Pore-forming Peptides and Protein Toxins* (Menestrina, G., Dalla Serra, M., and Lazarovici, P., eds) pp. 132–147, Taylor and Francis, London
9. Maček, P. (1992) *FEMS Microbiol. Immunol.* **105,** 121–130
10. Maček, P., and Lebez, D. (1981) *Toxicon* **19,** 233–240
11. Batista, U., Maček, P., and Sedmak, B. (1990) *Cell Biol. Int. Rep.* **14,** 1013–1024
12. Maček, P., Belmonte, G., Pederzolli, C., and Menestrina, G. (1994) *Toxicology* **87,** 205–227
13. Athanasiadis, A., Anderluh, G., Maček, P., and Turk, D. (2001) *Structure* (*Camb.*) **9,** 341–346
14. Hinds, M. G., Zhang, W., Anderluh, G., Hansen, P. E., and Norton, R. S. (2002) *J. Mol. Biol.* **315,** 1219–1229
15. Mancheño, J. M., Martín-Benito, J., Martínez-Ripoll, M., Gavilanes, J. G., and Hermoso, J. A. (2003) *Structure* (*Camb.*) **11,** 1319–1328
16. Malovrh, P., Viero, G., Dalla Serra, M., Podlesek, Z., Lakey, J. H., Maček, P., Menestrina, G., and Anderluh, G. (2003) *J. Biol. Chem.* **278,** 22678–22685
17. Gutiérrez-Aguirre, I., Barlič, A., Podlesek, Z., Maček, P., Anderluh, G., and González-Mañas, J. M. (2004) *Biochem. J.* **384,** 421–428
18. Anderluh, G., and Lakey, J. H. (2005) in *Protein-Lipid Interactions. From Membrane Domains to Cellular Networks* (Tamm, L. K., ed) pp. 141–162, Wiley-VCH, Weinheim, Germany
19. Anderluh, G., Barlič, A., Podlesek, Z., Maček, P., Pungerčar, J., Gubenšek, F., Zecchini, M. L., Dalla, S., and Menestrina, G. (1999) *Eur. J. Biochem.* **263,** 128–136
20. Malovrh, P., Barlič, A., Podlesek, Z., Maček, P., Menestrina, G., and Anderluh, G. (2000) *Biochem. J.* **346,** 223–232
21. Hong, Q., Gutiérrez-Aguirre, I., Barlič, A., Malovrh, P., Kristan, K., Podlesek, Z., Maček, P., Turk, D., González-Mañas, J. M., Lakey, J. H., and Anderluh, G. (2002) *J. Biol. Chem.* **277,** 41916–41924
22. Birck, C., Damian, L., Marty-Detraves, C., Lougarre, A., Schulze-Briese, C., Koehl, P., Fournier, D., Paquereau, L., and Samama, J. P. (2004) *J. Mol. Biol.* **344,** 1409–1420
23. Carrizo, M. E., Capaldi, S., Perduca, M., Irazoqui, F. J., Nores, G. A., and Monaco, H. L. (2005) *J. Biol. Chem.* **280,** 10614–10623
24. Gutiérrez-Aguirre, I., Trontelj, P., Maček, P., Lakey, J. H., and Anderluh, G. (2006) *Biochem. J.* **398,** 381–392
25. Bernheimer, A. W., and Avigad, L. S. (1976) *Proc. Natl. Acad. Sci. U. S. A.* **73,** 467–471
26. De los Ríos, V., Mancheño, J. M., Lanio, M. E., Oñaderra, M., and Gavilanes, J. G. (1998) *Eur. J. Biochem.* **252,** 284–289
27. Caaveiro, J. M., Echabe, I., Gutiérrez-Aguirre, I., Nieva, J. L., Arrondo, J. L., and González-Mañas, J. M. (2001) *Biophys. J.* **80,** 1343–135
28. Barlič, A., Gutiérrez-Aguirre, I., Caaveiro, J. M., Cruz, A., Ruiz-Argüello, M. B., Pérez-Gil, J., and González-Mañas, J. M. (2004) *J. Biol. Chem.* **279,** 34209–34216
29. Martin-Benito, J., Gavilanes, F., de Los Rios, V., Mancheño, J. M., Fernandez, J. J., and Gavilanes, J. G. (2000) *Biophys. J.* **78,** 3186–3194
30. Mancheño, J. M., Martín-Benito, J., Gavilanes, J. G., and Vázquez, L. (2006) *Biophys. Chem.* **119,** 219–223
31. Anderluh, G., Razpotnik, A., Podlesek, Z., Maček, P., Separovic, F., and Norton, R. S. (2005) *J. Mol. Biol.* **347,** 27–39
32. Kristan, K., Viero, G., Maček, P., Dalla, S. M., and Anderluh, G. (2007) *FEBS J.* **274,** 539–550
33. Bligh, E. G., and Dyer, W. J. (1959) *Can. J. Biochem. Physiol.* **37,** 911–917
34. Anderluh, G., Beseničar, M., Kladnik, A., Lakey, J. H., and Maček, P. (2005) *Anal. Biochem.* **344,** 43–52
35. Schlattner, U., and Wallimann, T. (2000) *J. Bioenerg. Biomembr.* **32,** 123–131
36. Meier, C., Aricescu, A. R., Assenberg, R., Aplin, R. T., Gilbert, R. J., Grimes, J. M., and Stuart, D. I. (2006) *Structure* (*Camb.*) **14,** 1157–1165
37. Schwede, T., Kopp, J., Guex, N., and Peitsch, M. C. (2003) *Nucleic Acids Res.* **31,** 3381–3385
38. Honig, B., and Nicholls, A. (1995) *Science* **268,** 1144–1149
39. DeLano, W. L. (2002) *The PyMOL Molecular Graphics System*, DeLano Scientific, Palo Alto, CA
40. Maček, P. (1983) *Structural and Functional Properties of Equinatoxins.* Doctoral dissertation, University of Ljubljana
41. Zecchini, M. (1994) *Struttura e Funzione du una Citolisina Basica Estratta dalle Nematocisti dell'Anemone di Mare Actina equina*. Master's thesis, Universita di Padova
42. Kahya, N., Scherfeld, D., Bacia, K., Poolman, B., and Schwille, P. (2003) *J. Biol. Chem.* **278,** 28109–28115
43. Veatch, S. L., and Keller, S. L. (2003) *Biophys. J.* **85,** 3074–3083
44. Jiang, X. Y., Yang, W. L., Chen, H. P., Tu, H. B., Wu, W. Y., Wei, J. W., Wang, J., Liu, W. H., and Xu, A. L. (2002) *Toxicon* **40,** 1563–1569
45. Belmonte, G., Pederzolli, C., Maček, P., and Menestrina, G. (1993) *J. Membr. Biol.* **131,** 11–22
46. Tejuca, M., Dalla Serra, M., Ferreras, M., Lanio, M. E., and Menestrina, G. (1996) *Biochemistry* **35,** 14947–14957

47. Jiang, X., Chen, H., Yang, W., Liu, Y., Liu, W., Wei, J., Tu, H., Xie, X., Wang, L., and Xu, A. (2003) *Biochem. Biophys. Res. Commun.* **312,** 562–570
48. De los Rios, I., Mancheño, J. M., Del Pozo, A. M., Alfonso, C., Rivas, G., Oñaderra, M., and Gavilanes, J. G. (1999) *FEBS Lett.* **455,** 27–30
49. Alegre-Cebollada, J., Rodriguez-Crespo, I., Gavilanes, J. G., and Del Pozo, A. M. (2006) *FEBS J.* **273,** 863–871
50. Meinardi, E., Florin-Christensen, M., Paratcha, G., Azcurra, J. M., and Florin-Christensen, J. (1995) *Biochem. Biophys. Res. Commun.* **216,** 348–354
51. Meyer, E. A., Castellano, R. K., and Diederich, F. (2003) *Angew. Chem. Int. Ed. Engl.* **42,** 1210–1250
52. Wimley, W. C., and White, S. H. (1996) *Nat. Struct. Biol.* **3,** 842–848
53. Ulmschneider, M. B., and Sansom, M. S. (2001) *Biochim. Biophys. Acta* **1512,** 1–14
54. de Planque, M. R., and Killian, J. A. (2003) *Mol. Membr. Biol.* **20,** 271–284
55. Hong, H., Park, S., Jimenez, R. H., Rinehart, D., and Tamm, L. K. (2007) *J. Am. Chem. Soc.* **129,** 8320–8327
56. Lomize, A. L., Pogozheva, I. D., Lomize, M. A., and Mosberg, H. I. (2007) *BMC Struct. Biol.* **7,** 44
57. Bavdek, A., Gekara, N. O., Priselac, D., Gutierrez, A., I., Darji, A., Chakraborty, T., Maček, P., Lakey, J. H., Weiss, S., and Anderluh, G. (2007) *Biochemistry* **46,** 4425–4437
58. Yamaji, A., Sekizawa, Y., Emoto, K., Sakuraba, H., Inoue, K., Kobayashi, H., and Umeda, M. (1998) *J. Biol. Chem.* **273,** 5300–5306
59. Stahelin, R. V., and Cho, W. (2001) *Biochemistry* **40,** 4672–4678
60. Stahelin, R. V., Digman, M. A., Medkova, M., Ananthanarayanan, B., Rafter, J. D., Melowic, H. R., and Cho, W. (2004) *J. Biol. Chem.* **279,** 29501–29512
61. Stahelin, R. V., Hwang, J. H., Kim, J. H., Park, Z. Y., Johnson, K. R., Obeid, L. M., and Cho, W. (2005) *J. Biol. Chem.* **280,** 43030–43038
62. Cho, W., and Stahelin, R. V. (2005) *Annu. Rev. Biophys. Biomol. Struct.* **34,** 119–151
63. Lee, S. A., Kovacs, J., Stahelin, R. V., Cheever, M. L., Overduin, M., Setty, T. G., Burd, C. G., Cho, W., and Kutateladze, T. G. (2006) *J. Biol. Chem.* **281,** 37091–37101
64. Blatner, N. R., Wilson, M. I., Lei, C., Hong, W., Murray, D., Williams, R. L., and Cho, W. (2007) *EMBO J.* **26,** 3709–3719
65. Poklar, N., Fritz, J., Maček, P., Vesnaver, G., and Chalikian, T. V. (1999) *Biochemistry* **38,** 14999–15008
66. Turk, T., Maček, P., and Gubenšek, F. (1989) *Toxicon* **27,** 375–384
67. Alegre-Cebollada, J., Lacadena, V., Oñaderra, M., Mancheño, J. M., Gavilanes, J. G., and Del Pozo, A. M. (2004) *FEBS Lett.* **575,** 14–18
68. Bonev, B. B., Lam, Y. H., Anderluh, G., Watts, A., Norton, R. S., and Separovic, F. (2003) *Biophys. J.* **84,** 2382–2392
69. Openshaw, A. E. A., Race, P. R., Monzo, H. J., Vazquez-Boland, J. A., and Banfield, M. J. (2005) *J. Biol. Chem.* **280,** 35011–35017
70. Ago, H., Oda, M., Takahashi, M., Tsuge, H., Ochi, S., Katunuma, N., Miyano, M., and Sakurai, J. (2006) *J. Biol. Chem.* **281,** 16157–16167
71. Tomita, T., Noguchi, K., Mimuro, H., Ukaji, F., Ito, K., Sugawara-Tomita, N., and Hashimoto, Y. (2004) *J. Biol. Chem.* **279,** 26975–26982
72. Kiyokawa, E., Makino, A., Ishii, K., Otsuka, N., Yamaji-Hasegawa, A., and Kobayashi, T. (2004) *Biochemistry* **43,** 9766–9773
73. Mahfoud, R., Garmy, N., Maresca, M., Yahi, N., Puigserver, A., and Fantini, J. (2002) *J. Biol. Chem.* **277,** 11292–11296